Nonflammable perfluoropolyether-based electrolytes for lithium batteries

Dominica H. C. Wong[a,1], Jacob L. Thelen[b,1], Yanbao Fu[c], Didier Devaux[c], Ashish A. Pandya[a], Vincent S. Battaglia[c], Nitash P. Balsara[b,c,d,2], and Joseph M. DeSimone[a,e,2]

[a]Department of Chemistry, University of North Carolina at Chapel Hill, Chapel Hill, NC 27599; [b]Department of Chemical Engineering University of California, Berkeley, CA 94720; [c]Environmental Energy Technologies Division and [d]Materials Science Division, Lawrence Berkeley National Laboratory, University of California, Berkeley, CA 94720; and [e]Department of Chemical and Biomolecular Engineering, North Carolina State University, Raleigh, NC 27695

Edited by Yushan S. Yan, University of Delaware, Newark, DE, and accepted by the Editorial Board December 30, 2013 (received for review August 8, 2013)

The flammability of conventional alkyl carbonate electrolytes hinders the integration of large-scale lithium-ion batteries in transportation and grid storage applications. In this study, we have prepared a unique nonflammable electrolyte composed of low molecular weight perfluoropolyethers and bis(trifluoromethane)sulfonimide lithium salt. These electrolytes exhibit thermal stability beyond 200 °C and a remarkably high transference number of at least 0.91 (more than double that of conventional electrolytes). Li/$LiNi_{1/3}Co_{1/3}Mn_{1/3}O_2$ cells made with this electrolyte show good performance in galvanostatic cycling, confirming their potential as rechargeable lithium batteries with enhanced safety and longevity.

fluorinated polymers | nonflammable electrolytes

Large-scale rechargeable batteries are expected to play a key role in today's emerging sustainable energy landscape (1, 2). State-of-the-art lithium (Li) batteries not only are used to power zero-emission electric vehicles, but they currently are gaining traction as backup power in aircraft and smart grid applications (3, 4). The electrolyte used in these batteries, however, hinders their use in large-scale applications: it contains a flammable mixture of alkyl carbonate solvents that frequently leads to safety issues. Dimethyl carbonate (DMC), an important component in commercial Li-ion battery electrolytes, has an HMIS (Hazardous Materials Identification System) flammability rating of 3 on a scale of 0–4, indicating a high risk of ignition under most operating conditions. The intrinsic instability of carbonate-based solvents worsens at higher temperatures, at which exothermic electrolyte breakdown often leads to thermal runaway (5, 6), resulting in catastrophic failure of the battery. Although this failure rate stands at about one in ten million systems, it is intolerable for large-scale applications in which cost and user safety might be heavily compromised. This necessitates the development of radically new electrolytes with improved safety.

Desirable electrolyte properties include a large window of phase stability (no vaporization or crystallization), complete nonflammability, a wide electrochemical stability window, and suitable ionic transport for the targeted application. There are many approaches to synthesizing materials with these properties, e.g., ionic liquids (7, 8), gel-polymer matrices (9, 10), and small molecule additives (11–13). Systems using poly(ethylene oxide) (PEO) also are well studied (14, 15). PEO can solvate high concentrations of lithium salts and is considered nonflammable. Unfortunately, practical conductivity often is limited within a high temperature range (14), and it is well known that in these systems, the motion of the Li ion carries only a small fraction of the overall current (also known as the Li-ion transference number, t^+). PEO-based electrolytes typically exhibit t^+ values between 0.1 and 0.5 (16–20), leading to strong salt concentration gradients across the electrolytes that limit power density. Recently, we reported the surprising miscibility of PEO with its perfluorinated analog, known as perfluoropolyethers (PFPEs) (21). Building upon this work, we found that various lithium salts were soluble not only in blends of PEO and PFPEs, but also directly in pure PFPEs.

Herein, we report the synthesis and characterization of a class of nonflammable liquid electrolytes for lithium batteries based on neat functionalized PFPEs. PFPEs are a class of fluoropolymers that remain as liquids over a large temperature range [glass transition temperatures (T_g) <−80 °C], exhibit low toxicity, and are extremely chemically resistant (22). Our approach was to use PFPEs as an intrinsically fireproof platform that can be chemically tailored to achieve the desired conductive properties for Li-ion batteries. We found that functionalized PFPEs can solvate the well-known bis(trifluoromethane)sulfonimide lithium salt (LiTFSI) and conduct Li ions with a high transference number close to unity. We demonstrate successful cycling of Li/$LiNi_{1/3}Co_{1/3}Mn_{1/3}O_2$ (LiNMC) cells with a PFPE/LiTFSI electrolyte, confirming the viability of using this material toward the development of inherently safe batteries.

Results and Discussion

Hydroxy-terminated PFPEs (PFPE-diols) with nominal molecular weights of 1,000, 1,400, 2,000, and 4,000 g/mol were purchased from Solvay. In addition to studying these materials, we modified the terminal groups of PFPE chains to more closely resemble chemistries that have been used successfully in batteries, thereby increasing compatibility with current battery systems. A one-step reaction with these oligomers and methyl chloroformate in the presence of triethylamine in 1,1,1,3,3-pentafluorobutane resulted in the formation of methyl carbonate-terminated PFPEs

Significance

This research article describes a unique class of nonflammable electrolytes for lithium-ion batteries that are based on functionalized perfluoropolyethers (PFPEs). It demonstrates that PFPEs may be used as a major component in operating batteries. These electrolytes not only are completely nonflammable, but they also exhibit unprecedented high transference numbers and low electrochemical polarization, indicative of longer battery life. The results in this work may represent a significant step toward a lithium-ion battery with improved safety and pave the way for the development of new electrolytes that can address the persisting challenges of current battery technologies.

Author contributions: D.H.C.W., J.L.T., D.D., N.P.B., and J.M.D. designed research; D.H.C.W., J.L.T., Y.F., and D.D. performed research; D.H.C.W., Y.F., A.A.P., and V.S.B. contributed new reagents/analytic tools; D.H.C.W., J.L.T., Y.F., N.P.B., and J.M.D. analyzed data; and D.H.C.W., J.L.T., D.D., N.P.B., and J.M.D. wrote the paper.

The authors declare no conflict of interest.

This article is a PNAS Direct Submission. Y.S.Y. is a guest editor invited by the Editorial Board.

[1]D.H.C.W. and J.L.T. contributed equally to the work.

[2]To whom correspondence may be addressed. E-mail: desimone@unc.edu or nbalsara@berkeley.edu.

This article contains supporting information online at www.pnas.org/lookup/suppl/doi:10.1073/pnas.1314615111/-/DCSupplemental.

A

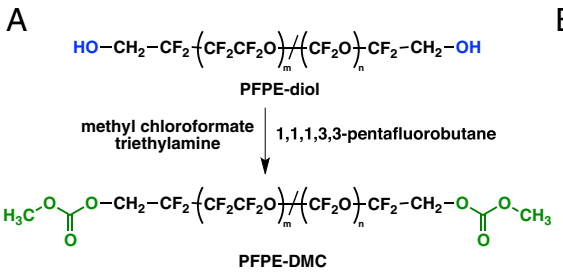

B

Electrolyte	DP	T_g (°C)
$PFPE_{1000}$-diol	10	-89
$PFPE_{1400}$-diol	13	-98
$PFPE_{2000}$-diol	24	-112
$PFPE_{4000}$-diol	48	-117
$PFPE_{1000}$-DMC	10	-95
$PFPE_{1400}$-DMC	13	-101
$PFPE_{2000}$-DMC	24	-113
$PFPE_{4000}$-DMC	48	-118

Fig. 1. PFPE oligomers as Li-ion electrolytes. (*A*) Chemical reaction scheme describing the synthesis of PFPE-DMC from PFPE-diol. (*B*) PFPE-diol and PFPE-DMC electrolytes with corresponding degrees of polymerization and glass transition temperatures.

(PFPE-DMCs) (Fig. 1*A*). The PFPEs studied are listed in Fig. 1*B*, along with the corresponding degrees of polymerization (DPs) (*SI Appendix*) and T_gs. PFPE-diols exhibit higher T_gs than their PFPE-DMC counterparts, owing to increased intermolecular attractions between chains caused by hydrogen bonding.

The flammability of electrolytes was evaluated based on their thermal stability, fire sustainability, and flash point. Fig. 2*A* shows the thermogravimetric (TG) curves of $PFPE_{1000}$-diol and $PFPE_{1000}$-DMC compared with pure DMC, its small molecule analog. DMC, a volatile liquid, experiences 5% weight loss at 34 °C (denoted as T_d), and 100% of the material was vaporized or degraded in the vicinity of 80 °C. In addition, DMC has a flash point below ambient temperatures (23) and can easily be ignited and sustain fire (Fig. 2*B*), posing both flammability and overpressurization hazards in lithium batteries. In contrast, $PFPE_{1000}$-diol and $PFPE_{1000}$-DMC demonstrate neither volatility nor thermal degradation below 200 °C; T_d values measured for these materials are 210 °C and 212 °C, respectively. Flash points also could not be detected for $PFPE_{1000}$-diol and $PFPE_{1000}$-DMC in our experimental window (25–200 °C), and they could not be ignited. Although the flash point of conventional lithium battery electrolytes (1:1 ethylene carbonate/DMC by volume) is 24 °C (24), slightly higher than that of DMC, the nonflammability and thermal stability of PFPEs nevertheless are more ideal, and can improve the safety of Li-ion batteries significantly.

Inductively coupled plasma mass spectrometry (ICPMS) was used to determine the solubility limit of LiTFSI in the PFPE electrolyte. Above this limit, salt precipitation occurs, leading to heterogeneous opaque mixtures (*SI Appendix*, Fig. S1). In Fig. 3*A*, we plot the maximum salt concentration in terms of molarity and r_{max}, where r is defined as the molar ratio of Li^+ ions to perfluoroalkylene oxide moieties in the chain, versus the nominal PFPE molecular weight. The relationship between both molarity and r_{max} and molecular weight for both PFPE-diols and PFPE-DMCs shows an exponential decay of LiTFSI loading as molecular weight increases. However, when salt concentration is normalized by the concentration of terminal groups and plotted as R_{max}, defined as the molar ratio of Li^+ ions to hydroxyl and methyl carbonate moieties (Fig. 3*A*, *Inset*), the maximum concentration is nearly independent of molecular weight. This analysis shows that the carbonate functionalization allows for nearly double the maximum salt loading relative to PFPE-diols, presumably because carbonate moieties interact more favorably with Li^+ than hydroxyl groups. To confirm our claim, IR spectroscopy was used to study the interactions between LiTFSI and PFPE polymers. Fig. 3*B* shows IR spectra of $PFPE_{1000}$-DMC blends with LiTFSI at various concentrations, compared with pure LiTFSI and $PFPE_{1000}$-DMC. A shift in the C = O signal at 1,770 cm^{-1} to lower wavelengths is observed as the LiTFSI concentration increases. The peak shifts systematically with increasing salt concentration and is at ~1,750 cm^{-1} when $r = 0.08$. This observation is attributed to interactions between the carbonate moieties and Li^+. In contrast, the addition of LiTFSI to $PFPE_{1000}$-diol has no discernible effect on the measured IR spectra (*SI Appendix*, Fig. S2). Although overlap of the signals from $PFPE_{1000}$-DMC and LiTFSI precludes the observation of LiTFSI peak shifts in this region as the salt is being solvated, the decreased intensities at 1,350 cm^{-1} in $PFPE_{1000}$-DMC/LiTFSI blends is consistent with the presence of dissociated Li^+ and $TFSI^-$ ions (25–27).

Ionic conductivities of various PFPE-diol and PFPE-DMC mixtures with LiTFSI at 30 °C, measured via ac impedance spectroscopy, are shown in Fig. 4. By plotting the conductivities as a function of normalized concentration r, we show that although

A

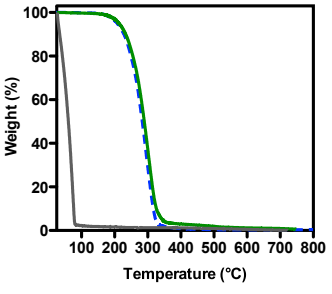

B

Electrolyte	T_d (5%)	Sustained Burning Time	Flash Point
DMC	34 °C	221 ± 7 s	18°C
$PFPE_{1000}$-diol	210 °C	No burning observed	None < 200°C
$PFPE_{1000}$-DMC	212 °C	No burning observed	None < 200°C

Fig. 2. Thermal stability and flammability of PFPEs. (*A*) TG curves for thermal decompositions of DMC (solid gray), $PFPE_{1000}$-diol (dashed blue), and $PFPE_{1000}$-DMC (solid green). (*B*) Corresponding decomposition temperature (5%), sustained burning characteristics, and flash points of these materials.

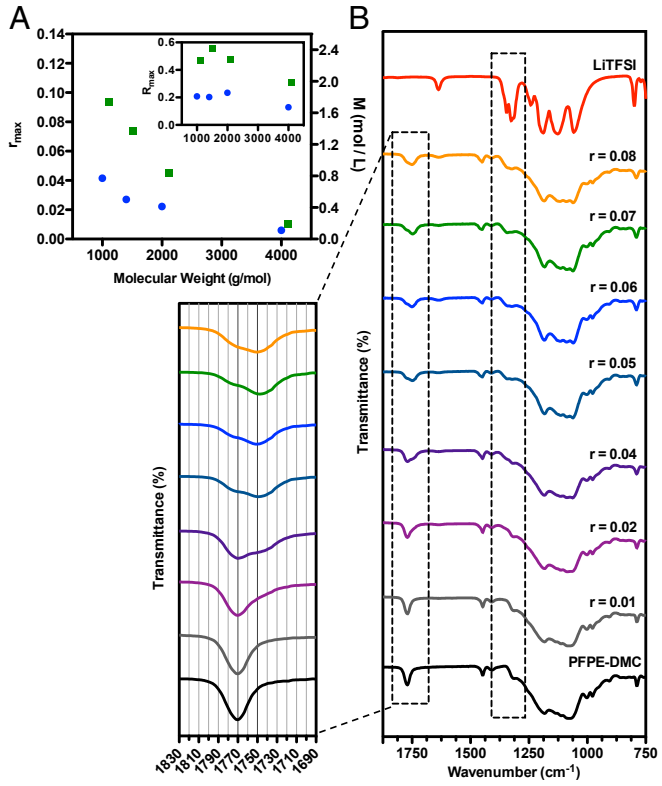

Fig. 3. Characterization of LiTFSI loading in PFPE electrolytes. (*A*) Maximum LiTFSI loading in PFPE-diols (blue) and PFPE-DMCs (green) expressed in r_{max}, the molar ratio of Li^+ ions to repeating fluoroether units and molarity, and in R_{max} (*Inset*), the molar ratio of Li^+ ions to end group functionalities, as a function of molecular weight. (*B*) IR spectra of $PFPE_{1000}$-DMC/LiTFSI blends at different concentrations.

end group composition heavily affects LiTFSI solvation, it does not influence ionic conduction significantly. All electrolytes appear to demonstrate a logarithmic dependence of conductivity on r that plateaus near $r = 0.08$. Analogous trends have been reported for structurally similar PEO electrolytes (28). In PEO systems, Li-ion transport is dictated predominantly by ion-chain interactions localized on the oligomer backbone, and the conductivity reaches a maximum at an LiTFSI concentration of around $r = 0.085$ (28, 29). It is important to note, however, that the conductivities of the PFPE systems tested are limited by their maximum salt loading, and no maximum in conductivity is observed. Thus, $PFPE_{1000}$-DMC, which can solvate the highest salt loading, is the most promising electrolyte among those tested, reaching a conductivity of 2.5×10^{-5} S·cm^{-1} at 30 °C. These conductivity values are significantly lower than that of conventional carbonate electrolytes (10^{-3} S/cm) but are comparable to that of PEO-based electrolytes at room temperature (4).

A more complete electrochemical characterization was performed on $PFPE_{1000}$-DMC at $r = 0.04$. Fig. 4*B* illustrates the temperature-dependent conductivity behavior of this electrolyte. We found that conductivity increases with increasing temperature, as is typical of macromolecular electrolytes. The Vogel–Tamman–Fulcher (VTF) equation, which typically is used to describe the dependence of viscosity on temperature near its T_g, also is used often to describe the temperature dependence of conductivity. It is expressed as

$$\sigma(T) = \frac{A}{\sqrt{T}} exp\left(\frac{-B}{R(T - T_0)}\right),$$

where σ is the ionic conductivity, A is a constant proportional to the number of charge carriers, B is equivalent to the activation energy for ion motion, R is the gas constant, T is the experimental temperature, and T_0 is an empirical reference temperature (30). It is clear from Fig. 4*B* that the conductivity of $PFPE_{1000}$-DMC is a weak function of temperature with $B = 0.47$ kJ·mol^{-1} (for a complete table of calculated VTF parameters, see *SI Appendix*, Table S1). This indicates a very low activation barrier for ion conduction. In fact, the measured conductivity at 120 °C is within a factor of 3 of that at 30 °C. The modest increase in conductivity with temperature and its thermal stability reduce the risk of detrimental side reactions that often are exothermic and lead to thermal runaway in conventional liquid Li-ion batteries.

In simple conductors with only one charged species, one observes Ohm's law in the limit of small dc potentials. The presence of two ions in electrolytes, however, generally results in large deviations from Ohm's law as the result of concentration polarization. To our surprise, we found that $PFPE_{1000}$-DMC/LiTFSI electrolytes at $r = 0.04$ exhibited behavior that was very close to that of a simple conductor. The electrolyte was sandwiched between two Li foil electrodes, and a steady potential of 0.02 V was applied for about 45 h at 38.8 °C. The electrolyte resistance (including both bulk and interfacial contributions) was measured at various times during the experiment by ac impedance.

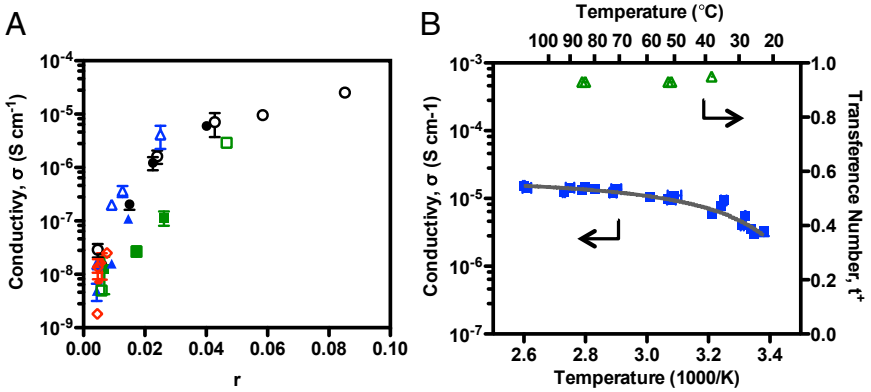

Fig. 4. Electrochemical behavior of PFPE electrolytes. (*A*) Ionic conductivities of $PFPE_{1000}$-diol (●), $PFPE_{1400}$-diol (green ■), $PFPE_{2000}$-diol (blue ▲), $PFPE_{4000}$-diol (red ◆), $PFPE_{1000}$-DMC (○), $PFPE_{1400}$-DMC (green □), $PFPE_{2000}$-DMC (blue △), and $PFPE_{4000}$-DMC (red ◇) with LiTFSI at 30 °C as a function of r. (*B*) t^+ (green △) and temperature-dependent conductivity (blue ■) of $PFPE_{1000}$-DMC. Conductivity follows VTF regression (gray, $A = 5.10^{-4}$ S·cm^{-1}·K$^{-0.5}$; $B = 0.47$ kJ·mol^{-1}, $T_0 = 271$ K).

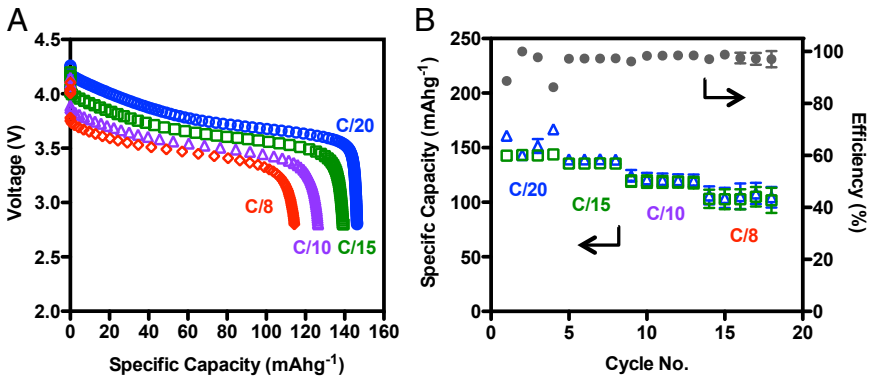

Fig. 5. Cyclability of Li/PFPE$_{1000}$-DMC-LiTFSI/LiNMC cells. (*A*) Discharge profiles obtained at 30 °C at different rates from C/20 to C/8 for a typical prototype Li/PFPE$_{1000}$-DMC-LiTFSI/LiNMC. (*B*) Cycle performance of battery prototypes showing discharge (green □) and charge (blue △) capacities, as well as overall efficiencies (gray ●).

The measured resistance after 6 h was 2,061.4 Ω/cm^2 and the measured current density, i_m, was 8.84 × 10^{-6} A·cm^{-2}. The expected current based on Ohm's law, i_o, is 9.70 × 10^{-6} A·cm^{-2}, i.e., i_m/i_o = 0.91. This implies that most of the current in our electrolyte is carried by the cation, i.e., the Li$^+$ transference number, t^+, a transport property that has a dramatic effect on battery performance, is in the vicinity of unity. Two approximate approaches were used to determine the transference number (*SI Appendix*, Figs. S3–S5). Both methods yield t^+ values between 0.91 and 1.0 in the temperature range of interest. To our knowledge, this is among the highest t^+ values reported for solutions containing lithium salts, and one of the few near-unity t^+ electrolytes with conductivities above 10^{-6} S/cm at room temperature. To establish the validity of our approaches for measuring t^+, we repeated our procedure using LiTFSI/polystyrene-PEO block copolymer electrolytes (where Li$^+$ is contained exclusively within the PEO block). The t^+ value of this electrolyte was about 0.12 (*SI Appendix*, Fig. S6), consistent with literature reports that t^+ values for LiTFSI/PEO electrolytes are between 0.1 and 0.3 (31, 32). In the future, we will use more rigorous approaches to measure t^+ (33). Although the relatively low conductivity of PFPE electrolytes may hinder power capacities, the near-unity transference number may mitigate some of these shortcomings: theoretical calculations show that materials with high t^+ values exhibit better battery performance than those possessing greater conductivity but a lower t^+ (34). The absence of polarization also reduces the risk of lithium plating and dendrite formation (31, 35). The Li-ion transference number of conventional carbonate electrolytes usually ranges between 0.1 and 0.5 (16); concomitant salt concentration gradients across the electrolyte limit battery life and power density. These t^+ values mainly are the result of strong interactions between oxygen atoms in the solvent molecules and lithium cations. We propose two possible reasons for our observation of a high transference number: (*i*) fluorine-containing functional groups on the PFPE backbone interact strongly with the fluorinated anion and reduce its mobility, and (*ii*) the delocalization of electron density caused by the fluorine moieties reduces the nucleophilicity of the oxygen atoms in the electrolyte, leading to their decreased binding strength to Li$^+$, facilitating cation transport across the medium. It is evident that both the PFPE main chain and the functional end groups play important roles in ion transport; conductivity at a given value of salt concentration is similar for widely different PFPE electrolytes (Fig. 4*A*), whereas salt solubility limits depend mainly on end group type and concentration (Fig. 3, *Inset*).

To investigate the viability of using PFPE electrolytes in lithium batteries, standard coin cell batteries were built using PFPE$_{1000}$-DMC at r = 0.04 as the electrolyte. Through cyclic voltammetry, we found that PFPE$_{1000}$-DMC is electrochemically stable up to 4.3 V (*SI Appendix*, Fig. S7), allowing for the use of high-voltage cathode materials, such as LiNMC. Lithium metal and LiNMC therefore were chosen as the anode and cathode, respectively. Cycling tests were performed at 30 °C at different charge rates (described as C/n, where n is the number of hours allotted to a full discharge of the theoretical cathode capacity "C"). Fig. 5*A* shows the typical discharge profiles of an Li/(PFPE$_{1000}$-DMC/LiTFSI)/LiNMC battery at C/20, C/15, C/10, and C/8. Capacities of 145, 140, 120, and 105 mA·h·g^{-1} were obtained at these respective rates. At C/10, the capacity of the same half-cell described in Fig. 5 replaced by a conventional carbonate-based electrolyte is 150 mA·h·g^{-1} (*SI Appendix*, Fig. S8). The results of successive cycling results at different C-rates (average behavior of four cells) are shown in Fig. 5*B*. The stable charge and discharge capacities for each C-rate indicate good compatibility between the PFPE and typical Li-ion battery cathode electrodes. Batteries that can be charged and discharged on the time scale of 8 h are immediately relevant to backing up solar panels. Therefore, further studies related to improving and optimizing electrolyte conductivity, rate capability, and testing battery performance under nonstandard temperature conditions are under investigation.

Conclusion

We have successfully demonstrated the use of PFPEs as a platform for the development of intrinsically safe lithium battery electrolytes. Designing electrolytes that solvate the fluorinated anion represents a radical departure from the established approach that is focused on solvating the lithium cation. By developing PFPE-DMC, we have incorporated compatibility with lithium salts in an inherently nonflammable material. The resulting electrolytes exhibit reasonable conductivity and unprecedented transference numbers. Their compatibility with standard battery electrodes provides the opportunity for seamless integration into current manufacturing infrastructure. Although much work remains to be done, we believe this work represents a significant step toward safer, high-energy lithium batteries and opens the door for the development of new electrolytes that can be tailored to address the persistent challenges of lithium-ion technologies.

Methods

Synthesis of PFPE-DMC. Fluorolink D10 and triethylamine were dissolved in 1,1,1,3,3-pentafluorobutane at 0 °C under stirring conditions and nitrogen atmosphere. A solution of methyl chloroformate dissolved in 1,1,1,3,3-pentafluorobutane then was added dropwise, after which the mixture was heated to 25 °C and stirred for 12 h. The resulting mixture was filtered under vacuum and washed with water three times and brine two times. The combined organic layers were dried over magnesium sulfate and filtered,

and the filtrate was evaporated under reduced pressure, giving the product $PFPE_{1000}$-DMC, as a pale yellow translucent liquid. ^1H NMR (400 MHz; chloroform; tetramethylsilane; ppm): $\delta = 3.87$ (s, 6 H), 4.52 (m, 4 H). This procedure was repeated with Fluorolink D10H, Fomblin ZDOL, and Fomblin ZDOL 4000 to produce $PFPE_{1400}$-DMC, $PFPE_{2000}$-DMC, and $PFPE_{4000}$-DMC, respectively.

Characterization of Electrolytes. All materials were dried in argon glove boxes with oxygen and water at sub-ppm levels for 24 h. Afterward, LiTFSI was added directly to PFPE samples and stirred at room temperature overnight. Li^+ concentration in PFPE electrolyte was determined using ICPMS after excess nonsolvated LiTFSI was removed through centrifugation. Thermogravimetric analysis (TGA) was performed using a PerkinElmer Pyris 1 TGA apparatus. A scan was made under nitrogen atmosphere from 20–600 °C with a heating rate of 10 °C/min. T_g, crystallization (T_c), and melting temperatures (T_m) were measured using a differential scanning calorimeter (DSC) (DSC Q 200; TA Instruments) in air using the method of heat/cool/heat at a heating and cooling rate of 10 °C/min and 5 °C/min, respectively, over a temperature range of −150 °C to 100 °C. The T_g was determined using the midpoint method on the second heating cycle thermogram. The T_c and T_m were determined as the peak maximum and minimum of the cooling and heating cycle, respectively. Sustained burning characteristics and flash point data were determined using a Rapid Flash Tester in accordance with American Society for Testing and Materials (ASTM) D4206 and ASTM D3278, respectively. IR spectroscopy was done using a Bruker ALPHA FT-IR instrument (from 500 to 4,000 cm^{-1} at a resolution of 4 cm^{-1}). Conductivity and cyclic voltammetry measurements were made via a 16-channel Bio-Logic VMP3 potentiostat. Cyclic voltammetry was conducted in Li metal/electrolyte/stainless steel standard coin cells. Conductivity measurements were obtained using a procedure similar to that previously reported by Teran et al. (36). Alternatively, conductivity may be calculated by impedance measurement of symmetric Li/Li cells. The ionic conductivity values reported for the symmetric lithium cells were calculated by normalizing the measured resistance by the volume of electrolyte in the porous separator:

$$\sigma = \frac{L}{RA\varepsilon}$$

where *L, R, A,* and ε are the length, resistance, cross-sectional area, and porosity of the separator, respectively.

Electrochemical Coin Cell Testing. Slurries containing 85.0 wt% lithium nickel manganese cobalt oxide (NMC), 7.0 wt% acetylene black, and 8.0 wt% polyvinylidene fluoride dispersed in N-methyl-2-pyrrolidone solvent were prepared. NMC laminates were prepared by casting the slurries onto aluminum foil by the doctor blade method. The laminates subsequently were punched into 14.3-mm diameter disks and dried completely before electrochemical studies. Active material loading is, on average, 1.9 mg/cm^2. Coin cells were assembled in standard 2325 coin cell hardware. Lithium foil was used as anode material, and NMC was used as active material in the cathode. Celgard 2500, punched into circles with a diameter of 20.6 mm, served as physical separators. The entire procedure was performed in an argon-filled glove box. Cell testing was conducted on a Maccor Battery Cycler connected to a Thermotron Environmental Chamber set at 30 °C. The batteries were cycled between 2.8 and 4.3 V with equivalent charge and discharge rates. Four formation cycles were performed at C/20 before the cycling rates were increased to C/15, C/10, and C/8, respectively.

ACKNOWLEDGMENTS. The work of D.H.C.W., A.A.P., and J.M.D. was funded by the Office of Naval Research (Grant N00014-10-10550 to J.M.D.) and the National Science Foundation (DMR-1122483). D.H.C.W. also is funded by the Natural Sciences and Engineering Research Council of Canada. A portion of this work was performed in the University of North Carolina (UNC) Energy Frontier Research Center (EFRC) Instrumentation Facility established by the UNC EFRC (Solar Fuels and Next Generation Photovoltaics, and EFRC funded by the US Department of Energy, Office of Science, Office of Basic Energy Sciences under Award DE-SC0001011) and the UNC Solar Energy Research Center Instrumentation Facility (funded by the US Department of Energy, Office of Energy Efficiency and Renewable Energy under Award DE-EE0003188). The work of J.L.T., Y.F., D.D., V.S.B., and N.P.B. is funded by the Assistant Secretary for Energy Efficiency and Renewable Energy, Office of Vehicle Technologies of the US Department of Energy under Contract DE-AC02-05CH11231 under the Batteries for Advanced Transportation Technologies Program.

1. Tarascon JM, Armand M (2001) Issues and challenges facing rechargeable lithium batteries. *Nature* 414(6861):359–367.
2. Goodenough JB, Park K-S (2013) The Li-ion rechargeable battery: A perspective. *J Am Chem Soc* 135(4):1167–1176.
3. Cheng FY, Liang J, Tao ZL, Chen J (2011) Functional materials for rechargeable batteries. *Adv Mater* 23(15):1695–1715.
4. Goodenough JB, Kim Y (2010) Challenges for rechargeable Li batteries. *Chem Mater* 22(3):587–603.
5. Hammami A, Raymond N, Armand M (2003) Runaway risk of forming toxic compounds. *Science* 301(5636):635–636.
6. Mandal BK, Padhi AK, Shi Z, Chakraborty S, Filler R (2006) Thermal runaway inhibitors for lithium battery electrolytes. *J Power Sources* 161(2):1341–1345.
7. Armand M, Endres F, MacFarlane DR, Ohno H, Scrosati B (2009) Ionic-liquid materials for the electrochemical challenges of the future. *Nat Mater* 8:621–629.
8. Lombardo L, Brutti S, Navarra MA, Panero S, Reale P (2013) Mixtures of ionic liquid—Alkylcarbonates as electrolytes for safe lithium-ion batteries. *J Power Sources* 227(0): 8–14.
9. Egashira M, Todo H, Yoshimoto N, Morita M (2008) Lithium ion conduction in ionic liquid-based gel polymer electrolyte. *J Power Sources* 178(2):729–735.
10. Song JY, Wang YY, Wan CC (1999) Review of gel-type polymer electrolytes for lithium-ion batteries. *J Power Sources* 77(2):183–197.
11. Wu L, et al. (2009) A new phosphate-based nonflammable electrolyte solvent for Li-ion batteries. *J Power Sources* 188(2):570–573.
12. Nagasubramanian G, Orendorff CJ (2011) Hydrofluoroether electrolytes for lithium-ion batteries: Reduced gas decomposition and nonflammable. *J Power Sources* 196(20): 8604–8609.
13. Naoi K, et al. (2009) Nonflammable hydrofluoroether for lithium-ion batteries: Enhanced rate capability, cyclability, and low-temperature performance. *J Electrochem Soc* 156(4):A272.
14. Croce F, Appetecchi GB, Persi L, Scrosati B (1998) Nanocomposite polymer electrolytes for lithium batteries. *Nature* 394:456–458.
15. Fergus JW (2010) Ceramic and polymeric solid electrolytes for lithium-ion batteries. *J Power Sources* 195(15):4554–4569.
16. Ghosh A, Wang C, Kofinas P (2010) Block copolymer solid battery electrolyte with high Li-ion transference number. *J Electrochem Soc* 157(7):A846–A849.
17. Capuano F, Croce F, Scrosati B (1991) Composite polymer electrolytes. *J Electrochem Soc* 138(7):1918–1922.
18. Appetecchi GB, Zane D, Scrosati B (2004) PEO-based electrolyte membranes based on $LiBC_4O_8$ salt. *J Electrochem Soc* 151(9):A1369–A1374.
19. Evans J, Vincent CA, Bruce PG (1987) Electrochemical measurement of transference numbers in polymer electrolytes. *Polymer (Guildf)* 28(13):2324–2328.
20. Watanabe M, Nishimoto A (1995) Effects of network structures and incorporated salt species on electrochemical properties of polyether-based polymer electrolytes. *Solid State Ion* 79(0):306–312.
21. Hu Z, et al. (2008) Optically transparent, amphiphilic networks based on blends of perfluoropolyethers and poly(ethylene glycol). *J Am Chem Soc* 139(43):14244–14252.
22. Rolland JP, Dam RMV, Schorzman DA, Quake SR, DeSimone JM (2004) Solvent-resistant photocurable "liquid Teflon" for microfluidic device fabrication. *J Am Chem Soc* 126(8):2322–2323.
23. Mikolajczak C, Kahn M, White K, Long RT *Lithium-Ion Batteries Hazard and Use Assessment* (Fire Protection Research Foundation, Massachusetts).
24. Hori M, Aoki Y, Maeda S, Tatsumi R, Hayakawa S (2010) Thermal stability of ionic liquids as an electrolyte for lithium-ion batteries. *ECS Trans* 25(36):147–153.
25. Huang W, Wheeler RA, Frech R (1994) Vibrational spectroscopic and ab initio molecular orbital studies of the normal and 13C-labelled trifluoromethanesulfonate anion. *Spectrochim Acta [A]* 50(5):985–996.
26. Rey I, Lassegues JC, Grondin J, Servant L (1998) Infrared and Raman study of the PEO-LiTFSI polymer electrolyte. *Electrochim Acta* 43:1505–1510.
27. Barteau KP, et al. (2013) Allyl glycidyl ether-based polymer electrolytes for room temperature lithium batteries. *Macromolecules* 46(22):8988–8994.
28. Panday A, et al. (2009) Effect of molecular weight and salt concentration on conductivity of block copolymer electrolytes. *Macromolecules* 42(13):4632–4637.
29. Lascaud S, et al. (1994) Phase diagrams and conductivity behavior of poly(ethylene oxide)-molten salt rubberyelectrolytes. *Macromolecules* 27(25):7469–7477.
30. Souquet J-L, Duclot M, Levy M (1996) Salt-polymer complexes: Strong or weak electrolytes? *Solid State Ion* 85(1–4):149–157.
31. Bouchet R, et al. (2013) Single-ion BAB triblock copolymers as highly efficient electrolytes for lithium-metal batteries. *Nat Mater* 12:450–457.
32. Edman L, Doeff MM, Ferry A, Kerr J, De Jonghe LC (2000) Transport properties of the solid polymer electrolyte system P(EO)nLiTFSI. *J Phys Chem B* 104(15):3476–3480.
33. Ma Y, et al. (1995) The measurement of a complete set of transport properties for a concentrated solid polymer electrolyte solution. *J Electroanal Chem* 142(6):1859–1868.
34. Doyle M, Fuller TF, Newman J (1994) The importance of the lithium ion transference number in lithium/polymer cells. *Electrochim Acta* 39(13):2073–2081.
35. Chazalviel JN (1990) Electrochemical aspects of the generation of ramified metallic electrodeposits. *Phys Rev A* 42(12):7355–7367.
36. Teran AA, Tang MH, Mullin SA, Balsara NP (2011) Effect of molecular weight on conductivity of polymer electrolytes. *Solid State Ion* 203:18–21.